RESEARCH ARTICLE / ARAŞTIRMA MAKALESİ

Dipole-Dipole Effect to Limits of Entanglement in Multipartite Spin Chain: A Monte Carlo Study

Çokparçalı Spin Zincirinde Dipol-Dipol Etkileşmesinin Dolaşıklığın Sınırlarına Etkisi: Monte Carlo Çalışması

İzzet Paruğ DURU[1] (ID), **Şahin AKTAŞ[2]** (ID)

[1]*İstanbul Gedik Üniversitesi, Tıbbi Görüntüleme Programı, 34722, İstanbul, Türkiye*
[2]*Marmara Üniversitesi, Fizik Bölümü, 34722, İstanbul, Türkiye*

Abstract
The entanglement of the ferromagnetically ordered isotropic spin-1/2 chain is discussed. The analytically deriving concurrence of a two-qubit state allows focusing on the effect of dipolar interaction (D). Low fields enable tuning creation/extinction of entangled states, particularly at low temperatures. There is a joint effect of the applied field and dipolar interaction which can't be disregarded. We perform Quantum Monte Carlo simulations on quantifying localizable entanglement (LE) in terms of upper/lower bounds. Findings reveal that D and B_z are decisive parameters on the production of entanglement including creation and extinction. A non-monotonic behavior has occurred under high fields at the critical temperature. However, strong D provides the stability of LE values concerning distance herewith conserving the unity at low temperatures under zero field. Rival regions are observed for the distant nearest neighbors, particularly odd ones.
Keywords: Dipole-dipole interaction, localizable entanglement, concurrence, loop algorithm, Monte Carlo method.

Öz
İzotropik ferromanyetik spin-1/2 zincirinde dolaşıklığın tartışıldığı bu çalışmada 2-kubit dolaşıklığının analitik çözümü yapılarak dipol-dipol etkileşmesine (D) odaklanılmıştır. Harici manyetik alan (B_z), özellikle düşük sıcaklıklarda, dolaşıklığın oluşumunu ve sönümlenmesini kontrol edebilmektedir. Kuantum Monte Carlo simülasyon metodu ile dolaşıklığın alt ve üst sınırları hesaplanarak dipolar etkileşme (D) de harici alanla (B_z) beraber dolaşıklığın oluşması ve yok olması sürecinde karar verici parametreler oldukları sonucuna varılmaktadır. Kritik sıcaklıkta ve yüksek manyetik alan altında monoton olmayan davranış ile karşılaşılmıştır. Ayrıca, uzak spinler arasındaki dolaşıklığın baskın dipolar etki ile kararlı hale geldiği ve düşük sıcaklıklarda 20 komşu spin ile hala dolaşık halde kalsada yüksek sıcaklıklarda uzak komşu dolaşıklığının eriminin azaldığı anlaşılmaktadır. Tek komşu spinler arasında "rival" bölgeler gözlenmektedir.
Anahtar Kelimeler: Dipol-dipol etkileşmesi, localize dolaşıklık, eşevrelilik, döngü algoritması, Monte Carlo metodu.

I. INTRODUCTION

Entanglement provides a remarkable aspect on performing quantum information processes such as teleportation [1, 2, and 3] and quantum computation [4, 5, 6, 7, and 8] providing a substantial resource of information [9]. Heisenberg and Ising-like models which describe the magnetic behavior of a solid-state system [10 and 11], have been commonly preferred to study entanglement and strong correlations due to its literal and simplistic structure. Furthermore, both experimental and theoretical investigations on behalf of magnetic characterization and spin correlations including simulation studies have been progressed with a broad perspective of researchers in the field reporting either miscellaneous or convergent results [12, 13, 14, 15, 16, 17, 18, and 19]. Previous works elaborately focused on Heisenberg Hamiltonian describing the quantum spin-1/2 chain, since 1D-spin arrays, greatly incorporating entangled states, can be introduced as a reliable candidate for quantum information processes [20, 21, 22, and 23]. They also focused on the concurrence of the system which refers to the mixed states of two-qubits. Wang studied thermal entanglement for isotropic XY model deducing that zero-field concurrence has unity for low temperatures up to temperature (T), T = 0.2 while it vanishes at T = 1.1 even if the external field (B) is applied [24]. However quantum phase transition at a critical value of B is observed at T = 0 for isotropic XY chain [25]. According to the calculations of Rigolin, entanglement vanished at T = 0.9 for isotropic XXX model (J = 1) [26]. Besides concurrence measurements of two nearest neighboring spins, the entanglement of multi-particle systems can provide practical information between long-ranged pairs of spins. LE is the most suitable measurement tool for this type of quest. Therefore, Androvitsaneas et.al, investigated the relation between LE and anisotropy of system for XY and XYZ model under external field and/or zero-field reporting singularities herewith resulting in a quantum critical point as $B_z = 0.75$. Moreover, revival regions are shown for the next nearest 10 neighbors [27] under certain magnetic fields and thermal agitations. Sinyagin et al., dressed spherical nanostructures with dipoles to determine the aggregation state of the system [28].

It can be confidently argued that long-distant stably entangled pairs procure a remarkable fact for topological storage [29]. However, the long-range entanglement of two-qubit is studied by [30] revealing the coupling of selected qubits with considerable distances. Additionally, various long-ranged inter-acted systems have a fabulous potential to study [31, 32, 33, 34, 35, 36, 37, 38, 39, 40, and 41]. In this manner, dipolar interaction between spins has been taken into consideration to deal with magnetic monopoles [34]. Several experimental studies have been performed to investigate the properties of quasiparticle excitations [39, 40, and 42] by treating low dimensional quantum-spin models. The first demonstration of entangled spins separated with 220 250A distance in a bulk material is evaluated by Sahling at very low temperatures [43]. In the theoretical aspect, quantum phase transitions should be clearly understood from the sight of quantum information in the area of condensed matter physics [44, 45, and 46]. Bravo et al. emphasized the significance of dipolar interactions on antiferromagnetic spin chains under transverse magnetic field stressing a quantum phase transition [46]. Previously, we have focused on a spin-chain ordered as AFM considering dipolar interaction (D) and external magnetic field (B) observing rival regions related to the temperature for certain D and B values [47].

This study brings out the effect of dipole-dipole interaction (D) to upper and lower limits of entanglement in isotropic ferromagnetic spin-1/2 Heisenberg chain under uniform external magnetic field (B_z) along the z-axis. LE is a suitable tool to investigate entanglement in multipartite systems via quantifying bipartite entanglement. Hence, it indicates the maximized entanglement between two parts of the system on average by carrying local measurements out the rest of the system [51]. Concurrence and thermal entanglement of two-qubit Heisenberg Hamiltonian including dipolar interaction is well measured respectively, before evaluating LE based on the calculation of correlation functions (Q_{ij}). Loop algorithm, embedded in ALPS package [48], is used to determine LE [49 and 50] in terms of upper and lower bounds. Note that LE is related to the entanglement of assistance (EoF). Simulation data is post-processed by a Phyton script developed by the authors. We aimed not only to deal with the effect of dipolar interaction on entanglement both analytically and numerically but also to quantify the entanglement of the distant spins (long-ranged) in multipartite systems.

In Section 2, Hamiltonian of the spin chain and the procedure of calculating expectation values applying loop algorithm with Quantum Monte Carlo methodology were explained. Thermal entanglement of two-spin as two-qubits state was investigated via concurrence analytically in Section 3.1. Section 3.2 focused on localizable entanglement determining the

upper and lower bounds considering temperature, spin-spin length, strength of the dipolar interaction and external magnetic field. Results were summarized in Section 4.

II. MODEL

The Hamiltonian of the N-qubit one-dimensional spin chain with dipole-dipole interaction term and magnetic field along z-direction is given by,

$$\hat{\mathcal{H}} =$$

$$-\sum_{i=1}^{N}\left[J_x\hat{\sigma}_i^x\hat{\sigma}_{i+1}^x + J_y\hat{\sigma}_i^y\hat{\sigma}_{i+1}^y + J_z\hat{\sigma}_i^z\hat{\sigma}_{i+1}^z + B_z(\hat{\sigma}_i^z)\right] + \hat{\mathcal{H}}_D \quad (1)$$

$$\hat{\mathcal{H}}_D = \frac{D}{2}\sum_{i=1}^{N}\left[\frac{\hat{\sigma}_i\hat{\sigma}_{i+1}}{r_{i\,i+1}^3} - 3\frac{(\hat{\sigma}_i.r_{i\,i+1})(\hat{\sigma}_{i+1}.r_{i\,i+1})}{r_{i\,i+1}^5}\right] \quad (2)$$

where $J_\alpha(\alpha: x, y, z)$ are exchange coupling constants, B_z denotes magnetic field along z-axis and D represents the strength of dipole interaction (r_{ij}: two-spin distance vector) in dipolar Hamiltonian $\hat{\mathcal{H}}_D$. Only nearest neighboring spin, interactions are taken into account, in which periodic boundary conditions (PBC) are satisfied $\sigma_1 = \sigma_{N+1}$. A clear illustration of the model is given in Figure 1.
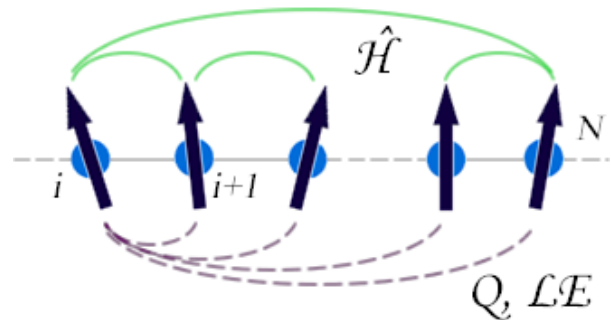
Figure 1. Illustration of spin chain: Green narrow and wide rounded lines represent the interacted spin pairs and PBC, respectively, while purple dashed lines are used to specify the spin pairs

Various measurement techniques such as entanglement witness, concurrence, negativity, entanglement entropy help us to quantify entanglement. Moreover, thermal entanglement provides plenty of worthy pipelines, in which entanglement can be related to temperature. Therefore, we found an analytical solution of interested Hamiltonian (including dipolar term) that is operative for the two-qubit state, calculating density matrix, $\tilde{\rho}$.

We are interested in LE since it is a clear way to determine maximum entanglement between two parts of the system by measuring the rest parts locally. However, a tight relation has been built up among classical correlations and entanglement phenomena. Popp et al. proposed a primrose path to quantify entanglement in terms of upper and lower bounds. The latter is related to the classical two-point correlation function. According to Popp et al., the correlation function can be described as [51],

$$Q_{\alpha\beta}^{ij}(|\psi\rangle\langle\psi|) = \langle\psi|\hat{\sigma}_\alpha^i \otimes \hat{\sigma}_\beta^j|\psi\rangle - \langle\psi|\hat{\sigma}_\alpha^i|\psi\rangle\langle\psi|\hat{\sigma}_\beta^j|\psi\rangle \quad (3)$$

In spin-1/2 systems, a connection between concurrence and LE can be generalized to higher-dimensional spin systems, realized by unrolling the equation $LE_{ij}(\psi) \geq max | Q_{\alpha\beta}^{ij}(\psi) |$ for a given pure state $|\psi\rangle$ of N qubits. The right side of the inequality belongs to the lower bound of entanglement (LE_{ij}^{lb}). On the other hand, the upper bound is revealed by using entanglement of assistance (EoA). Thus, the bounds of entanglement can be easily described by the following equation.

$$max\left(|Q_{xx}^{ij}|, |Q_{yy}^{ij}|, |Q_{zz}^{ij}|\right) \leq LE_{i,j} \leq \frac{\sqrt{x_+^{ij}} + \sqrt{x_-^{ij}}}{2} \quad (4)$$

Note that, the right side of the equation represents the upper bound of the entanglement (LE_{ij}^{ub}).

$$x_\pm^{ij} = \left(1 \pm \langle\sigma_z^i\sigma_z^j\rangle\right)^2 - \left(\langle\sigma_z^i\rangle \pm \langle\sigma_z^j\rangle\right)^2 \quad (5)$$

As a substantial way to simulate quantum spin systems loop algorithms introduce a powerful methodology based on clustering spins on discrete imaginary time. In contrast to the traditional Markov Chain Monte Carlo (MCMC), the Markov process presents a continuous cycle in transition probabilities between the spin (S) and graph configurations (G). Introducing spin-1/2 lattice with exchange coupling interactions and Heisenberg Hamiltonian of the model has been followed by the simulation process. Applying loop algorithm by lowering the temperature with small steps during thermalization to decrease long equilibration times. Thermalization cost 10^3 of Monte Carlo steps

before the measurement process of physical quantities. Here we focused on the energy as a function of temperature based on the generalization of clustering process updating spin system (MC updates). Suzuki-Trotter decomposition was used to obtain a path-integral representation of Z and weight of world-line graphs C (W(C)).

$$Z = \sum_C W(C)P(C) \quad (6)$$

P is the projection operator evolving C during imaginary time direction and a continuous imaginary time scheme was chosen. The weight P(C) is related to the projection operator; note that, W(C) is the counterpart of the path-integral picture of our model constructed on our Hamiltonian. Certain spin configurations and plaquettes in which a group of spins is pictured in graphs and flipping spins by a probability. This process is also consistent with a detailed balance condition. A transition probability of spins in chosen plaquette leads to break-ups forming clusters through the loop. New spin configurations can be created by spin flipping in a cluster with a probability (shown in Figure 2). A detailed description of the loop algorithm can be found in [52].

The $Q_{\alpha\beta}^{ij}$ and $X_\pm^{ij}$ are calculated with the aid of simulated data. We performed QMC simulations with parallel processing for parameters D, kT and B_z, *exampli grati*, at a temperature scale $kT \in (0,4]$. This corresponds to a large number of physical conditions. Obtaining the expected value of an A observable, it is crucial to represent through an estimator related to the W(C).

$$< A >= \frac{\sum_C A(C)W(C)}{\sum_C W(C)} \quad (7)$$
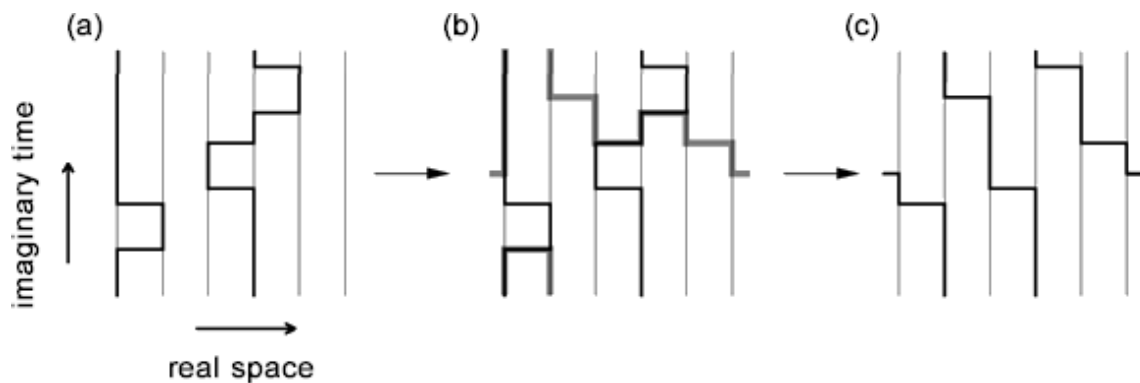
Figure 2. Evolution of spins in space: A set of spin flips draw the spin orientations in graphs along the continuous imaginary-time direction. Three arbitrary pictures at the end of several spin flips are given in (a), (b), and (c).

III. FINDINGS AND DISCUSSION

3.1 .Thermal entanglement of two-qubit ground state

In the case of spin-1/2 chain including an only nearest-neighbor dipolar interaction term, Heisenberg Hamiltonian operator of bipartite spin system takes the form as expressed in Equation (8) where r denote

distance between spins, and D is related to dipolar constant.

$$\hat{\mathcal{H}} = -\left(\frac{J_x}{2} + \frac{D}{r^3}\right)\hat{S}_1^x\hat{S}_2^x + \left(\frac{D}{2r^3} - \frac{J_y}{2}\right)\hat{S}_1^y\hat{S}_2^y$$

$$+ \left(\frac{D}{2r^3} - \frac{J_z}{2}\right)\hat{S}_1^z\hat{S}_2^z - \frac{B_z}{2}\left(\hat{S}_1^z + \hat{S}_2^z\right) \quad (8)$$

J_x, J_y and J_z represent exchange couplings where negative (positive) values/sign corresponds to FM

(AFM) interaction; $\hat{\sigma}_\alpha^\beta$ are known as Pauli spin matrices operating to up/down spin in the basis $|\uparrow\uparrow\rangle, |\uparrow\downarrow\rangle, |\downarrow\uparrow\rangle$, $|\downarrow\downarrow\rangle$. For simplicity (to operate $\hat{H}$ easily), we reorganized $\hat{H}$ in terms of raising and lowering operators, $\hat{S}^\pm = \hat{\sigma}^x \pm i\hat{\sigma}^y$.

$$\hat{H} = \left(-\frac{3D}{2r^3} - \frac{J_x}{2} + \frac{J_y}{2}\right)(\hat{\sigma}_1^+\hat{\sigma}_2^+ + \hat{\sigma}_1^-\hat{\sigma}_2^-)$$
$$+ \left(-\frac{D}{2r^3} - \frac{J_x}{2} - \frac{J_y}{2}\right)(\hat{\sigma}_1^+\hat{\sigma}_2^- + \hat{\sigma}_1^-\hat{\sigma}_2^+) \quad (9)$$
$$+ \left(\frac{D}{2r^3} - \frac{J_z}{2}\right)\hat{\sigma}_1^z\hat{\sigma}_2^z - \frac{B_z}{2}(\hat{\sigma}_1^z + \hat{\sigma}_2^z)$$

Matrix form of the $\hat{H}$ were given in Equation (10) with a worthy reduced format since we only handled the isotropic ferromagnetic state where $J_\alpha = J$; herewith γ and τ are set to $\frac{D}{2r^3} - \frac{J}{2}$ and $-\frac{3D}{2r^3}$ respectively.

$$\hat{H} = \begin{bmatrix} \gamma - B_z & 0 & 0 & \tau \\ 0 & -\gamma & -\gamma - \frac{3J}{2} & 0 \\ 0 & -\gamma - \frac{3J}{2} & -\gamma & 0 \\ \tau & 0 & 0 & \gamma + B_z \end{bmatrix} \quad (10)$$

Eigenvalues and corresponding eigenstates of the Hamiltonian (Equation (10)) used to calculate the density matrix of the interested system, were given in Table 1, where $\eta^+ = (\epsilon^2 + 1)^{-1/2}$ and $\eta^- = (\delta^2 + 1)^{-1/2}$ are normalization constants, while $\epsilon = \frac{(B_z^2 + \tau^2)^{1/2} - B_z}{\tau}$ and $\delta = -\frac{(B_z^2 + \tau^2)^{1/2} + B_z}{\tau}$.

Table 1. Eigenvalues and corresponding eigenvectors of $\hat{H}$

Eigenvalues	Eigenvectors
$E_1 = \gamma + (B_z^2 + \tau^2)^{1/2}$	$\|\psi_1\rangle = \eta^+(\epsilon \|\uparrow\uparrow\rangle + \|\downarrow\downarrow\rangle)$
$E_2 = \gamma - (B_z^2 + \tau^2)^{1/2}$	$\|\psi_2\rangle = \eta^-(\delta \|\uparrow\uparrow\rangle + \|\downarrow\downarrow\rangle)$
$E_3 = \frac{3J}{2}$	$\|\psi_3\rangle = \frac{1}{\sqrt{2}}(\|\uparrow\downarrow\rangle - \|\downarrow\uparrow\rangle)$
$E_4 = -\frac{3J}{2} - 2\gamma$	$\|\psi_4\rangle = \frac{1}{\sqrt{2}}(\|\uparrow\downarrow\rangle + \|\downarrow\uparrow\rangle)$

The density matrix of the system, $\tilde{\rho}$ can be constructed by $\tilde{\rho} = \frac{\sum_{i=1}^4 e^{-\beta E_i}|\psi_i\rangle\langle\psi_i|}{Z}$ where $Z = Tr[e^{-\beta\hat{H}}]$. For a pair of qubits, average of entanglement of density matrix $\tilde{\rho}$ is a monotonically increasing function of the concurrence C. When C = 1 we have maximally entangled states and when C = 0 we do not have entanglement.

Concurrence can be calculated by $C \equiv max(0, \lambda_1 - \lambda_2 - \lambda_3 - \lambda_4)$, where λ_i is equal to the square roots of eigenvalues of $V_\rho = \tilde{\rho}(\sigma_1^y \otimes \sigma_2^y)\widetilde{\rho^*}(\sigma_1^y \otimes \sigma_2^y)$. The asterisk denotes complex conjugate. If $C = 1$, the state is maximally entangled else if $C = 0$, it is disentangled, while concurrence values of $(0, 1)$ interval indicates the strength of entanglement.

$$\tilde{\rho} = \begin{bmatrix} u & 0 & 0 & v \\ 0 & x & y & 0 \\ 0 & y & x & 0 \\ v & 0 & 0 & w \end{bmatrix} \quad (11)$$

$$u = \frac{1}{Z}\left(\frac{\epsilon^2}{\epsilon^2+1}e^{-\beta(\gamma+\epsilon\tau+B_z)} + \frac{\delta^2}{\delta^2+1}e^{-\beta(\gamma-\epsilon\tau-B_z)}\right)$$
$$v = \frac{1}{Z}\left(\frac{\epsilon}{\epsilon^2+1}e^{-\beta(\gamma+\epsilon\tau+B_z)} + \frac{\delta}{\delta^2+1}e^{-\beta(\gamma-\epsilon\tau-B_z)}\right)$$
$$w = \frac{1}{Z}\left(\frac{1}{\epsilon^2+1}e^{-\beta(\gamma+\epsilon\tau+B_z)} + \frac{1}{\delta^2+1}e^{-\beta(\gamma-\epsilon\tau-B_z)}\right) \quad (12)$$
$$x = \frac{1}{Z}e^{\beta\gamma}\cosh\left(3\beta\frac{J}{2} + \beta\gamma\right)$$
$$y = \frac{1}{Z}e^{\beta\gamma}\sinh\left(3\beta\frac{J}{2} + \beta\gamma\right)$$

Partition function, $Z = 2[e^{\gamma\beta}\cosh(1.5\beta J + \gamma\beta) + e^{-\gamma\beta}\cosh(\eta\tau + B_z)]$. Square roots of eigenvalues of V_ρ and concurrence were calculated numerically by setting $J = 1$. Note that B_z, D, and T possess real numbers as $B_z\epsilon(0,5), D\epsilon(0,4), T\epsilon(0,2)$.

$$\tilde{V}_\rho = \begin{bmatrix} uw^* + vv^* & 0 & 0 & uv^* + vu^* \\ 0 & xx^* + yy^* & xy^* + yx^* & 0 \\ 0 & xy^* + yx^* & xx^* + yy^* & 0 \\ vw^* + wv^* & 0 & 0 & vv^* + wu^* \end{bmatrix} \quad (13)$$

The state is disentangled under zero-field (B=0) in the FM case [53]. When the applied field is strengthened the number of $|\uparrow\uparrow\rangle$ states increases with inhibiting the creation of entanglement. There is no magnetic and thermal entanglement achieved for a two-qubit state when $D = 0$. That's why we focused on the effect of dipolar interaction. We intriguingly encountered that concurrence vanished in the absence of external field by numerical calculation, even if dipolar interaction has been taken into account. Concurrence vanished for high temperatures which depend on strength of the applied field. Low field (B_z=0.5) yielded a creation/extinction behavior (non-monotonicity) particularly originated from distinct dipolar strengths at certain low temperatures such as T=0.5 (Figure 3). However, strong D eliminated the hashing influence of temperature (Figure 4(a) and Figure 4(b)). Entanglement can be controlled via both D and T tuning entangled/disentangled states especially under slightly applied fields.
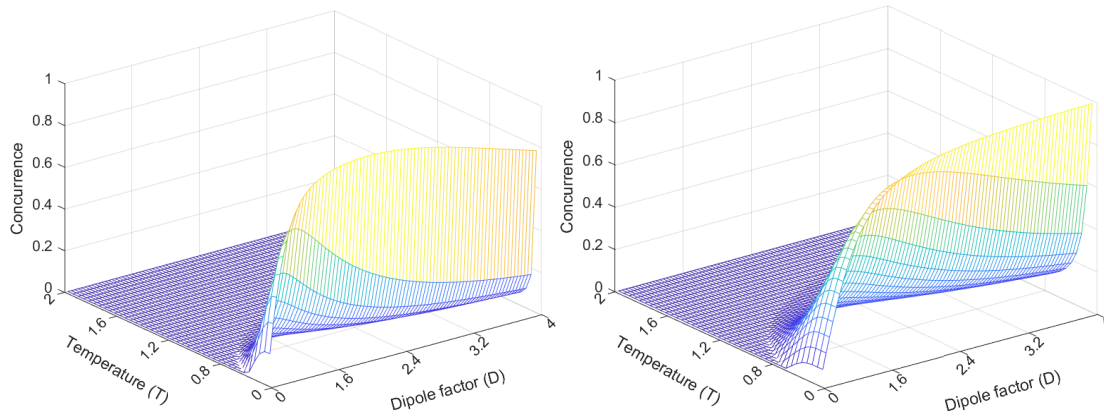
Figure 3. Concurrence as a function of temperature (T) and D for certain external magnetic fields (a) B=0.5 (b) B=1.
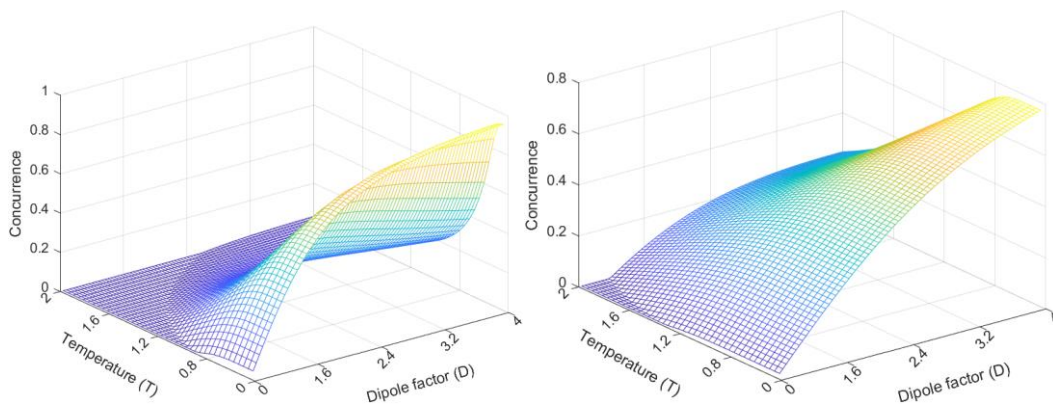
Figure 4. Concurrence as a function of temperature (T) and D for certain external magnetic fields (a) B=2 (b) B=5.

3.2. Localizable entanglement, upper and lower bounds: A Monte Carlo study

QMC simulations were performed to depict the bounds of LE for spin-1/2 particles spatially separated by identical distances. 2E+6 of steps are used for thermalization while 2E+7 sweeps were sufficient. We dealt with $L = 40$ spin ensuring the system can be approximated as an infinite chain. Findings of thermodynamic quantities (magnetization, energy) of XY and XYZ models are compared with existing results both analytical and numerical ones in the absence of dipole-dipole interaction.

Exchange coupling constants; J_x, J_y and J_z are set as $J_\alpha = 1$ ($\alpha = 0,1,2$) during the simulation process for the ferromagnetic isotropic model. We began by neglecting the dipole-dipole term ($D = 0$) to investigate the effect of both exchange and Zeeman interactions. Bounds of entangled pairs are determined in the absence of external magnetic field, under zero/low fields ($B_z = [0,0.5]$), relatively low/strong fields ($B_z = (0.5,2]$), and strong fields ($B_z = (2,5]$). Note that a strong external magnetic field enhancing the Zeeman term should dominate the rest by imposing the single spin to be aligned along its direction. It also affects the bound values since LE measurements have been predicated to two spin and single spin expectations. Moreover,

exchange and dipolar interactions spontaneously specify two-qubit states in parallel with correlations which are also calculated by mentioned expectation values. In this study, although exchange coupling constants have been set to unity, we assigned values to dipolar constant D and external field B_z to satisfy the relative dominancy of every interaction.

Results of firstlings indicate that LE_{ij}^{lb} has the lowest values under zero-field (Figure 5(a)); on the contrary, LE_{ij}^{ub} preserved unity for the entire temperature regime (Figure 5(b)). When the exchange interaction is only the commander of spins, the lower bound of entanglement between nearest neighbors (LE_{ij}^{lb}) has the lowest values for all temperatures (kT) as $kT \in (0,4]$. On the other hand, LE_{ij}^{ub} is maximized under zero-field. Moreover, it has not been affected via increasing temperature and remains almost unchanged. According to Figure 5, LE_{ij}^{lb} is increased by strengthing the applied field as Arnesen et al. have already reported [20]. $B_z = 0.5$, $B_z = 1$ and zero-field lower bound entanglement values started to overlap for $kT > 2$. However LE_{ij}^{ub} is lowered by the strong field herewith an increasing trend started at $T = 0.75$ prominently. Bounds of two nearest qubits are explicitly directed by B_z under certain temperatures in the absence of dipolar term.
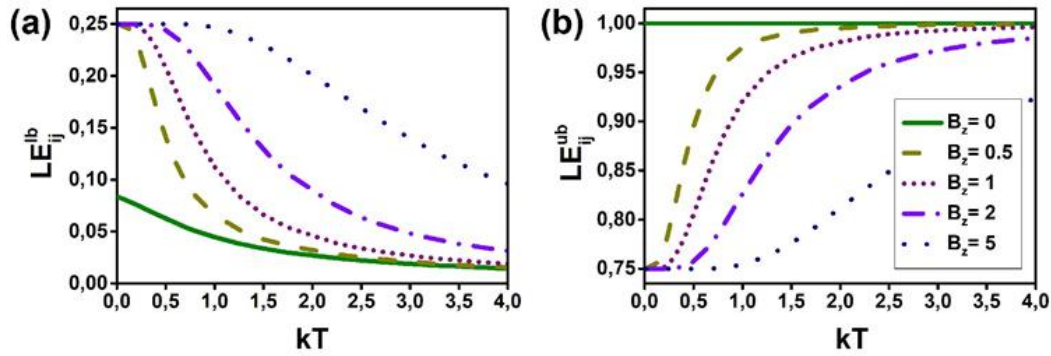
Figure 5. (a) LE_{ij}^{lb} and **(b)** LE_{ij}^{ub} as a function of temperature under $B_z = 0.5$, $B_z = 1$, $B_z = 2$, $B_z = 5$ and zero-field.
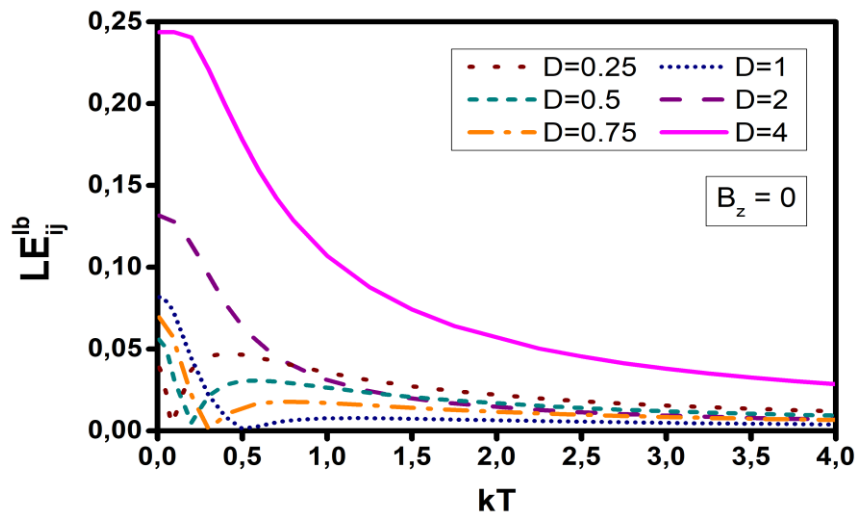
Figure 6. LE_{ij}^{ub} as a function of temperature for certain D strengths in the absence of an external field.

We now focused on the zero-field case for $N = 40$ spin-1/2 system incorporating the dipolar interaction strengthened by the times of dipole-dipole constant D. LE_{ij}^{ub} remains unchanged under thermal agitations since increasing temperature should not seduce the upper bound measured via two-spin and single spin expected values on the z basis (not shown here). Note that it is exactly not related to the observations of the x and y basis. As already stated, low-temperature values of the upper bound have an ascending trend under higher magnetic fields either for ferromagnetic or antiferromagnetic cases. On the other hand, Figure 6 shows that LE_{ij}^{lb} decreases monotonically via increasing temperature for every $D > 1$. However, we observed a non-linear change on values of LE_{ij}^{lb} by increasing kT when the strength of dipolar interaction diminishes for $D <= 1$. Besides, the lower bound has distinct critical kT values which impose the spin pairs to become untangled for $D = 1$, herewith $D \in \{0.25, 0.5, 0.75, 1\}$ point to the singularities of the system. LE_{ij}^{lb} of $D = 1$ vanishes at $kT = 0.5$ and afterwards entanglement of two-qubit is created at $kT > 0.5$ having lowest values unchanged. Additionally, $D = 0.75$ points a similar condition at temperature $kT = 0.3$. Furthermore, LE_{ij}^{lb}, increases while D values are increasing monotonically at $kT \to 0$ and $B_z = 0$.

Figure 7 displays the conduct of LE_{ij}^{lb} (a) and LE_{ij}^{ub} (b) under $B_z = 0.5$ magnetic field. LE_{ij}^{lb} shows a decreasing behavior via increasing temperature kT for whole D strengths except $D = 4$. LE_{ij}^{lb} is lowered whereby increasing D values up to $D = 2$. In contrast, $D = 4$, strong dipolar interaction implicitly pulls up the lower bound above $D = 0.25$ curve. That is to say dipolar term dominates the system below high temperatures since reasonable high temperatures assure lower bound values to overlap. $LE_{ij}^{lb} = 0.16 (D = 1)$, $LE_{ij}^{lb} = 0.07 (D = 2)$ and others have nearly the same value as 0.25, shortly, resulting in distinct lower bound values at kT that stands very close to $kT \to 0$. Upper bound, LE_{ij}^{ub} reaches unity for all D strengths at $kT > 2$. Upper bound converges to unity for $D = 2$ and $D = 4$ at all temperatures. A linear relation exists for all D values, adversely to the lower bound, under $B_z = 0.5$. Therefore LE_{ij}^{ub} of $D = 4$ is not significantly influenced by thermal agitations conserving almost unity. LE_{ij}^{lb} vanishes at $kT = 1.7$ and converges to zero for $D = 2$ under external magnetic field $B_z = 1$.
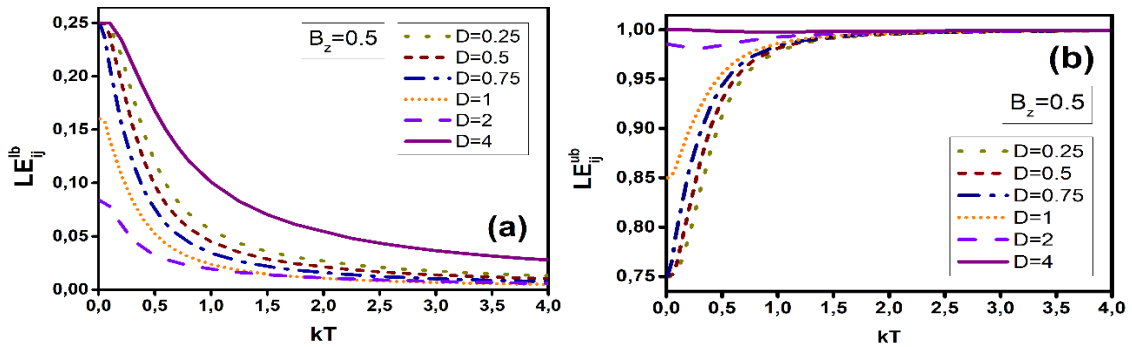
Figure 7. (a) LE_{ij}^{lb} and (b) LE_{ij}^{ub} as a function of temperature for certain D strengths under $B_z = 0.5$.
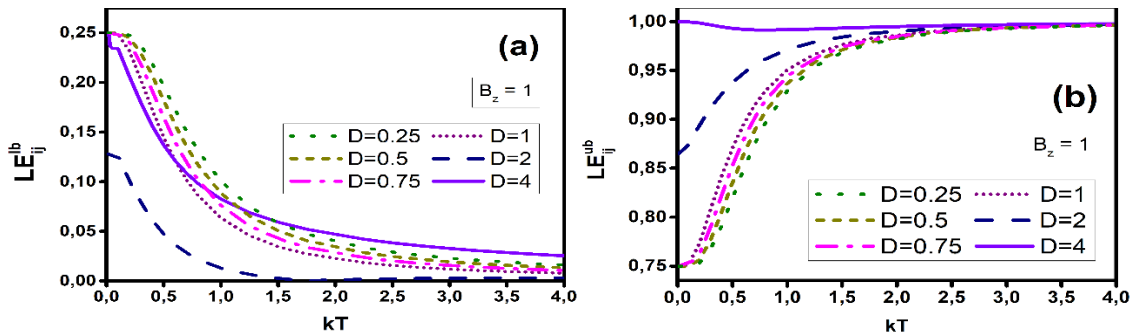
Figure 8. (a) LE_{ij}^{lb} and (b) LE_{ij}^{ub} as a function of temperature for certain D strengths under $B_z = 1$.

Besides, entanglement never disappears for the rest strengths of D's although LE_{ij}^{lb} shows a decrement trend through increasing temperature kT under magnetic field $B_z = 1$. In the same manner, LE_{ij}^{lb} decrease via increasing dipolar strength between $D \in \{0.25, 0.5, 0.75, 1, 2\}$. The behavior of LE under $B_z = 0.5$ (see Figure 7) and $B_z = 1$ (see Figure 8) are very similar but $D = 4$ values are getting lowered for latter case. At low temperatures LE_{ij}^{lb} takes value between $D = 2$ and $D = 1$ but they intersect with $D = 0.25, 0.5, 0.75$ and $D = 1$ values one by one at different temperatures having higher values rather than the others at temperatures as $kT > 1.75$. According to Figure 8(b), LE_{ij}^{ub} exhibits the similar behavior as if $B_z = 0.5$ applied. In other words, it directly increases via increasing dipolar strength under $B_z = 1$.

Thus far, the non-linear behavior of strong dipolar interaction $D = 4$ exists under relatively low magnetic fields ($B_z < 2$). We calculated values of lower and upper bounds under higher magnetic fields $B_z > 1$ to figure out if this behavior is dependent on the external magnetic field or not. Figure 8(a) and Figure 9 (a) displays LE_{ij}^{lb} values obtained under $B_z = 1$ and $B_z = 2$ external fields, respectively. A critical point as $kT = 0.5$ which entanglement vanishes even though neighboring spins entangle again for $kT > 0.5$ is indicated under $B_z = 2$. Moreover, LE_{ij}^{lb} values decrease via increasing dipolar constant D under magnetic field $B_z = 2$ but only immediately after a sharp drop entanglement vanished and entangled pairs emerge for $kT > 0.5$. LE_{ij}^{ub} shows similar behavior as stated for lower magnetic fields. The only difference is

strong dipolar interaction, briefly, $D = 4$, lead upper bound to lost unity. LE_{ij}^{lb} decrease by increasing temperature under $B_z = 2$. However, they diverge to zero at higher kT temperatures (increasing kT). Strong applied field inhibited to vanish entanglement at higher kT values.

$B_z = 5$ strictly regulated the upper and lower bounds, especially LE_{ij}^{lb}, inducing a monotonic behavior according to D strengths (see Figure 10). LE_{ij}^{lb} shows a descending behavior via increasing D values with non-vanishing character whereas non-unity values of LE_{ij}^{ub} increases by ascending D values. However, the bounds preserve temperature-related behavior as is under $B_z = 0.5, 1, 2$ although $D = 4$ violates it indicating a critical point at $kT = 0.5$. Zeeman term dominates the exchange interaction so classical correlations which have been calculated by two-spin and single spin expected values become directly dependent on the single spin measurement.

However, dipolar term loose efficiency is directly related to the distance of two spins in the lattice. In this manner, it will be dominated as exchange interaction even if distance-induced fluctuations exist. These fluctuations affect the system at certain temperatures for relatively weak fields ensuring critical points. Figure 11 summarizes the B-T relation of the lower limit between nearest neighboring spins for D values from $D = 1$ to $D = 4$ ($D < 1$ plot not shown in the text). According to Figure 11(c) ($D = 4$), there is non-monotonic LE_{ij}^{lb} values pointing "revival regions" at low temperatures under low magnetic fields.
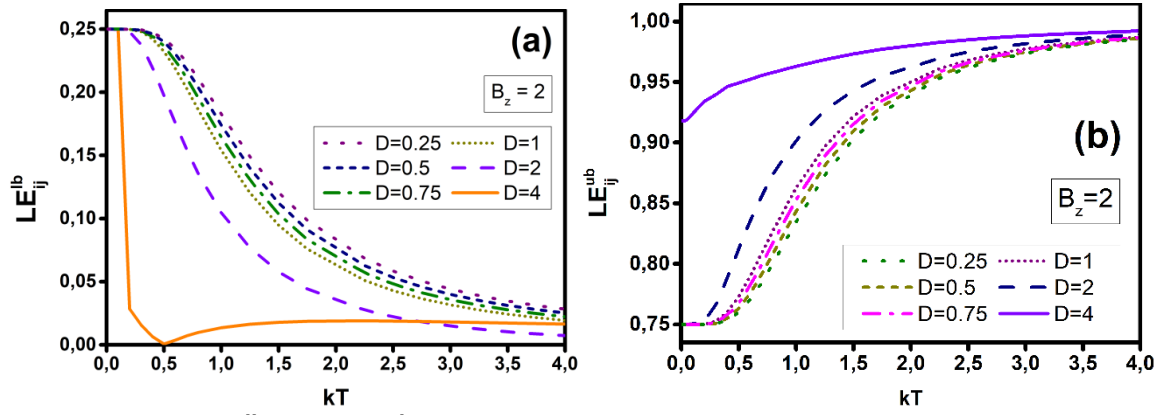
Figure 9. (a) LE_{ij}^{lb} and (b) LE_{ij}^{ub} as a function of temperature for certain D strengths under $B_z = 2$.
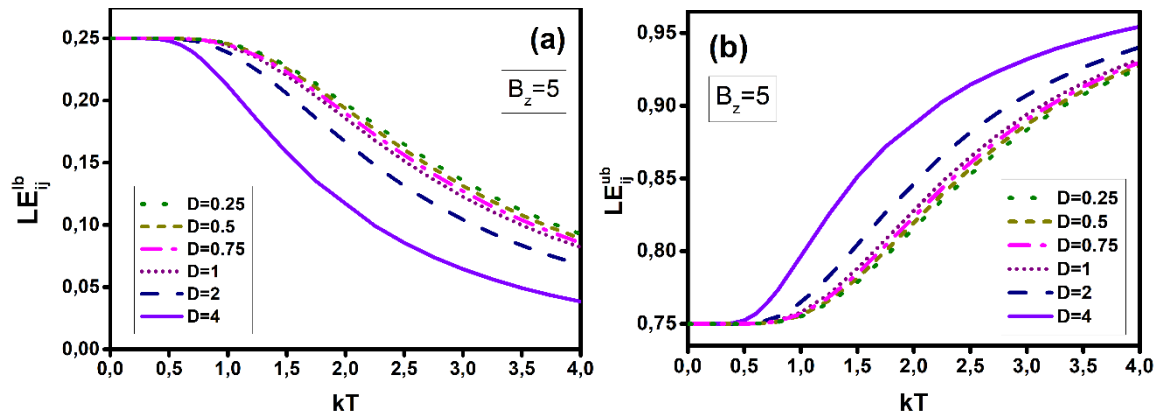
Figure 10. (a) LE_{ij}^{lb} and (b) LE_{ij}^{ub} as a function of temperature for certain D strengths under $B_z = 5$.
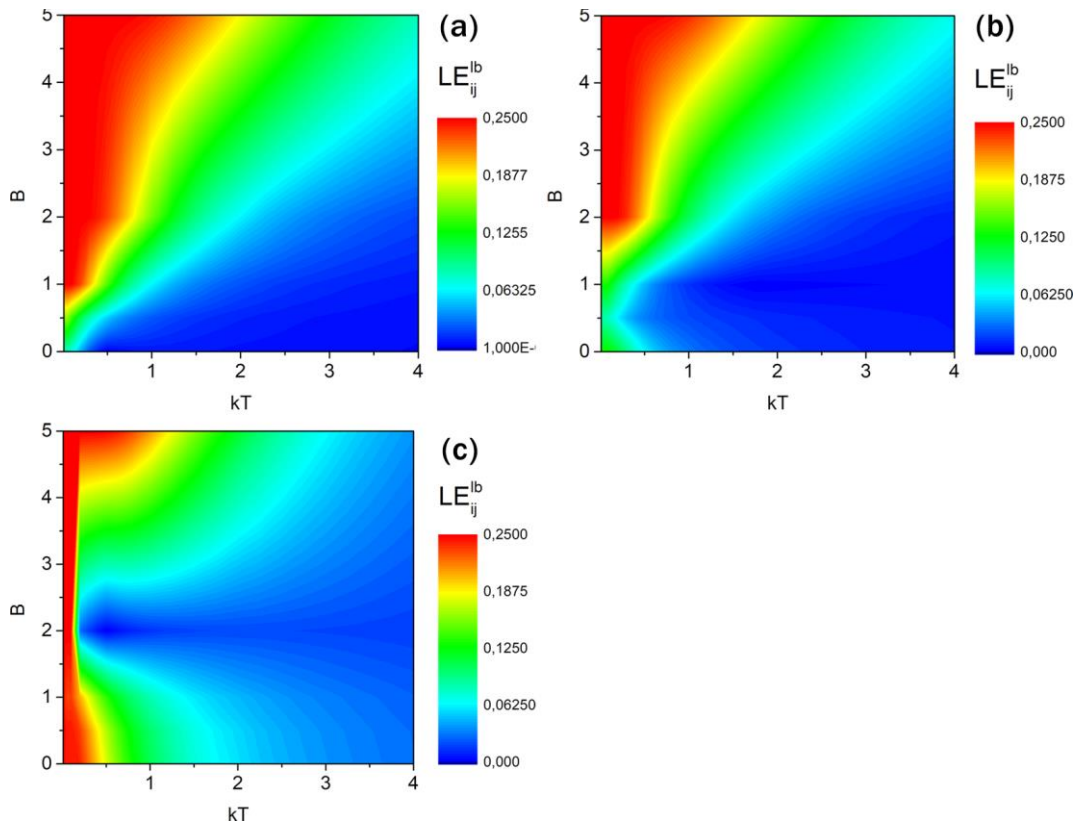
Figure 11. LE_{ij}^{lb} between two spin as a function of temperature and magnetic field B_z for (a) D = 1 (b) D = 2 (c) D=4.

Lower limits are calculated up to the 20th nearest neighbors to investigate the distance-dependent behavior of LE_{ij}^{lb} at certain temperatures in which dipolar interaction is included or not. Figure 12(a) displays the zero-field ($B_z = 0$) $LE_{ij}^{lb}(n)$ values corresponding to the latter circumstance ($D = 0$). n denotes the nth nearest neighboring spin where $j = i + n$ and $n = 20$. At very low-temperature regime as $kT = 0.05$, $LE_{ij}^{lb}(n)$ never vanishes for any neighboring spins in the absence of dipolar interaction and external magnetic field herewith having the lowest values (Figure 12(a)). $LE_{ij}^{lb}(n)$ showed a similar behavior in case of $D = 4$ counter to $D = 1$ and $D = 2$. Furthermore, increasing temperature tell us $LE_{ij}^{lb}(n)$ vanishes as well as dipolar interaction has been included. According to Figure 12 (d), $LE_{ij}^{lb}(n)$ remained unchanged with possessing similar values.

The dipolar interaction controls both the range and value of the lower bound namely $LE_{ij}^{lb}(n)$ between two spins of the ferromagnetic isotropic chain. Increasing temperature also influences the range of entanglement via agitating the spins thermally since they start to get over the domination of interactions included in the Hamiltonian of the spin-chain. One can deduce that the tightest quantum correlation between the spins would be induced by exchange and dipolar interactions in the absence of an external field. $LE_{ij}^{lb}(n)$ disappears farther in from the second nearest neighboring spin for the dipolar strengths $D = 1$(Figure 12 (b)) and the third nearest neighboring spin $D = 2$ (Figure 12 (c)) at temperatures $kT >= 0.5$.

Qi et al. obtained an analytical lower bound of concurrence by multi-qubit monogamy inequality for four-qubit quantum systems [54]. After a while, lower bounds were improved to achieve a more sensitive entanglement measure for $2x2x2^2$ mixed systems by [55]. A monogamous relation for upper bound was discussed including tripartite entanglement of the three-qubit system and multipartite concurrence earlier in the last decade [56]. The existence of long-ranged distant entangled qubits under zero magnetic field has great importance on the quantum information process. Nevertheless, the creation and extinction of entanglement at certain values of either kT and B_z depict critical points of the quantum system. We particularly analyzed distant dependent behavior of the lower bound only at $kT = 0.5$ (see Figure 13 (a)) and $kT = 0.05$ (see Figure 13 (b)) for $D = 0$, $D = 1$, $D = 2$ and $D = 4$ under zero field. At first sight, we must stress the loss of unity at higher temperature $kT = 0.5$ even though long-ranged entanglement has been conserved.
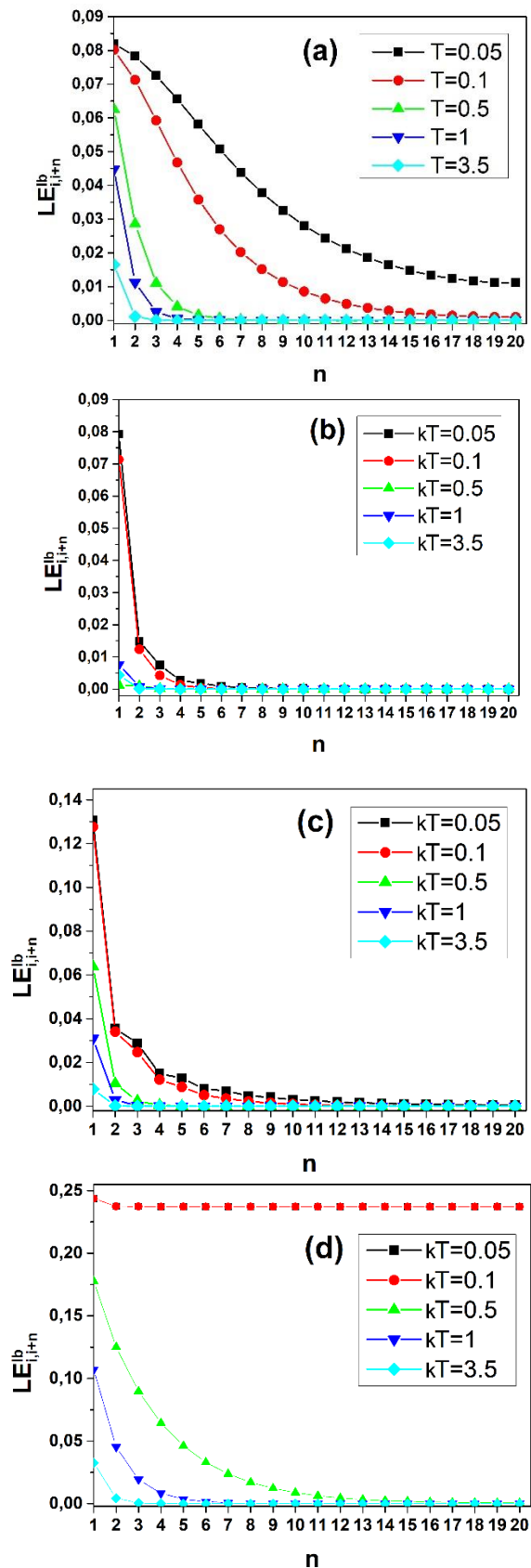
Figure 12. LE_{ij}^{lb} at temperatures kT = 0.05, kT = 0.1, kT = 0.5, kT = 1 and kT = 3.5 under zero field **(a)** D = 0 **(b)** D = 1 **(c)** D = 2 **(d)** D = 4.

It is a critical point in this study where the non-monotonic behavior of entanglement exists in the case of the special conditions mentioned above. According to Figure 13 (a), $LE_{ij}^{lb}(n)$ of nearest neighbouring qubits has a higher value for $D = 2$ and $D = 4$ than $D = 0$ though $D = 2$ stands very close to $D = 0$ at $kT = 0.5$. Both cases reveal that strengthening dipolar interaction provides highly entangled long-ranged pairs and also thermal agitations reduce the distance which qubits should communicate.
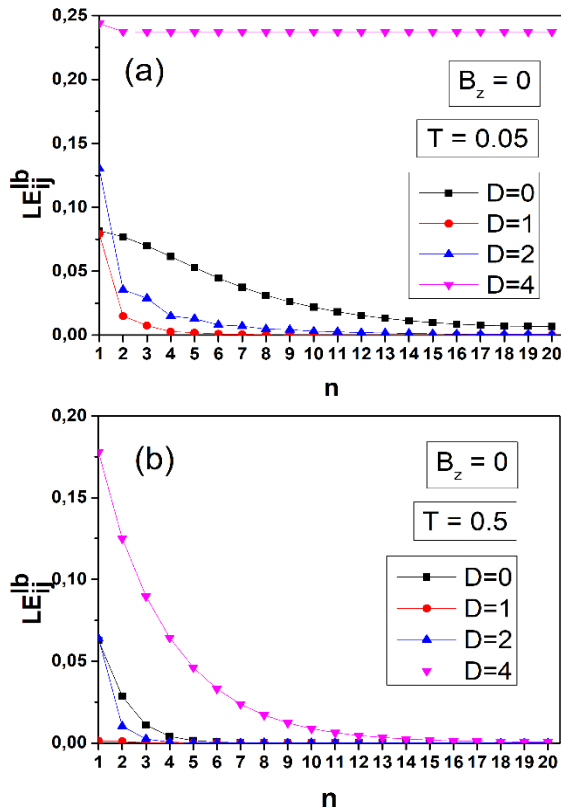
Figure 13. (a) LE_{ij}^{lb} (b) LE_{ij}^{ub} as a function of temperature for certain D strengths under zero field.

In addition, Figure 14 revealed the rival regions for distant odd sites for $n > 1$ under $B_z = 1$ at a low-temperature regime. We did not observe a clear non-monotonic behavior extinction-creation of entangled paired of distanced sites $n > 1$ pointing rival regions at certain temperatures. At very low temperatures as $kT \rightarrow 0$, LE_{ij}^{lb} a long-ranged maximized entanglement exists for $D = 4$ which was also stated. It was previously verified that a strong dipolar interaction (D) enhances long-ranged entanglement explicitly under zero-field unless high temperatures drastically reduced the amount of entanglement and range of communication in an AFM order. In contrast, localizable entanglement showed a non-linear dependency to D as detailed above. This text tried to clarify the effect of magnetic dipolar interaction in a spin system since direct dipole-dipole coupling not only provides valuable structural information but also takes a noteworthy place in modeling the magnetic resonance imaging process.
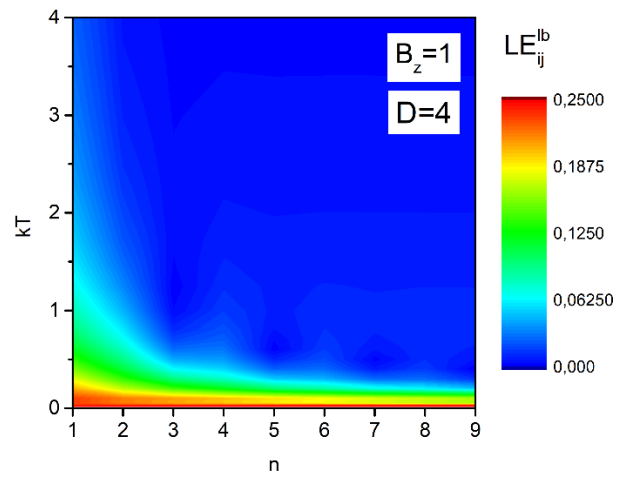
Figure 14. LE_{ij}^{lb} as a function of the distance between sites n and temperature for $D=4$ under $B_z = 1$.

IV. CONCLUSION

The concurrence of a spin-1/2 chain, ordered as FM, was analytically obtained to study thermal entanglement between two qubits. Low field ($B = 0.5$) yielded an extinction/creation behavior (non-monotonicity) that particularly originated from distinct dipolar strengths at certain low temperatures. We revealed upper and lower bounds to measure entanglement between any two parts of the multipartite system. According to QMC simulations, we found that the lower bound shows an increasing trend monotonically by strengthening the applied field when dipole-dipole interaction is neglected. Dipolar interaction affected the spin-1/2 chain, relative to the strength of D, both for nearest neighbor and distant qubits inducing a non-monotonic attitude. A rival region is observed for $D = 4$ under $B = 2$ magnetic field at $kT = 0.5$ in addition to $D = 0.25$, $D = 0.5$, $D = 0.75$ and $D = 1$ (at $kT = (0.5)$) in the absence of an external magnetic field. Moreover, strong dipolar interaction generated rival regions for distant odd sites for $n > 1$ under magnetic field $B = 1$ at low temperatures. In case of $B_z = 5$, lower bound which is the actual reflection of entanglement, decreased by increasing temperature since high magnetic field dominates spin orientation along field direction regarding to the considered temperature range. Besides, dominant external field led the entanglement lowered by increasing dipolar strength (D). Long-range entanglement that should be arranged in eligible solid systems ensures a non-fragile quantum correlation as a prominent tool for the quantum information process.

REFERENCES

[1] Modławska, J., & Grudka, A., (2008). Nonmaximally Entangled States Can Be Better for Multiple Linear Optical Teleportation. *Physical Review Letters, 100, 110503.*

[2] Cavalcanti, D., Skrzypczyk, P., & Šupić, I., (2017).All Entangled States can Demonstrate Nonclassical Teleportation. *Physical Review Letters, 119, 110501.*

[3] Z.A.Sabegh, R., & Mahmoudi, M., (2018). Spatially dependent atom-photon entanglement. *Scientific Reports, 8, 13840.*

[4] Loss, D., & DiVincenzo, D., (1998). Quantum computation with quantum dots. *Physical Review A, 57, 120.*

[5] Jürgen Audretsch (2007), The Quantum Computer. In Entangled Systems: New Directions in Quantum Physics *(pp.219-245), Weinheim, Germany: John Wiley and Sons, Ltd.*

[6] Belsley, M. (2014). Introduction to Quantum Information Science, by Vlatko Vedral. *Contemporary Physics, 55, 124.*

[7] DiVincenzo, D. (1997). Quantum computation and spin physics (invited). *Journal of Applied Physics, 81, 4602-4607.*

[8] Zheng, S., & Guo, G., (2000). Efficient Scheme for Two-Atom Entanglement and Quantum Information Processing in Cavity QED. *Physical Review Letters, 85, 2392-2395.*

[9] Bennett, C., & DiVincenzo, D., (2000). Quantum information and computation. *Nature, 404, 1476-4687.*

[10] Eggert, S., Affleck, I., & Takahashi, M., (1994). Susceptibility of the spin 1/2 Heisenberg antiferromagnetic chain. *Physical Review Letters, 73, 332-335.*

[11] Hammar, P., Stone, M., Reich, D., Broholm, C., Gibson, P., Turnbull, M., Landee, C., & Oshikawa, M., (1999). Characterization of a quasi-one-dimensional spin-1/2 magnet which is gapless and paramagnetic for g μ B H ≲ J and $k_B T \ll$ J. *Physical Review B, 59, 1008-1015.*

[12] Androvitsaneas, P., Fytas, N., Paspalakis, E., & Terzis, A.F., (2012). Quantum Monte Carlo simulations revisited: The case of anisotropic Heisenberg chains. *Philosophical Magazine, 92, 4649-4656.*

[13] Barma, M., & Shastry, B., (1978). Classical equivalents of one-dimensional quantum-mechanical systems. *Physical Review B, 18, 3351-3359.*

[14] Handscomb, D. (1964). A Monte Carlo method applied to the Heisenberg ferromagnet. *Mathematical Proceedings of the Cambridge Philosophical Society, 60, 115-122.*

[15] Harada, K., & Kawashima, N., (2001). Loop Algorithm for Heisenberg Models with Biquadratic Interaction and Phase Transitions in Two Dimensions. *Journal of the Physical Society of Japan, 70, 13-16.*

[16] Huang, Y., & Su, G., (2017). Quantum Monte Carlo study of the spin-1/2 honeycomb Heisenberg model with mixed antiferromagnetic and ferromagnetic interactions in external magnetic fields. *Physical Review E, 95, 052147.*

[17] Sandvik, A., & Kurkijärvi, J., (1991). Quantum Monte Carlo simulation method for spin systems. *Physical Review B, 43, 5950-5961.*

[18] Deger, C., Aksu, P., & Yildiz, F., (2016). Effect of Interdot Distance on Magnetic Behavior of 2-D Ni Dot Arrays. *IEEE Transactions on Magnetics, 52, 1-4.*

[19] Duru, I., Değer, C., Kalaycı, T., & Arucu, M., (2015). A computational study on magnetic effects of $Zn_{1-x}Cr_xO$ type diluted magnetic semiconductor. *Journal of Magnetism and Magnetic Materials, 396 pp. 268-274.*

[20] Arnesen, M., Bose, S., & Vedral, V., (2001). Natural Thermal and Magnetic Entanglement in the 1D Heisenberg Model. *Physical Review Letters, 87, 017901.*

[21] Marchukov, O.V., & Zinner, N., (2016). Quantum spin transistor with a Heisenberg spin chain. *Nature Communications, 7, 13070.*

[22] Renes, J., Miyake, A., Brennen, G., & Bartlett, S., (2013). Holonomic quantum computing in symmetry-protected ground states of spin chains. *New Journal of Physics, 15, 025020.*

[23] Apollaro, T., Lorenzo, S., Sindona, A., Paganelli, S., Giorgi, G., & Plastina, F., (2015). Many-qubit quantum state transfer via spin chains. *Physica Scripta, T165 pp. 014036.*

[24] Wang, X., (2002). Threshold temperature for pairwise and many-particle thermal entanglement in the isotropic Heisenberg model. *Physical Review A, 66, 044305.*

[25] Wang, X., (2001). Entanglement in the quantum Heisenberg XY model. *Physical Review A, 64, 012313.*

[26] Rigolin, G., (2004). Thermal entanglement in the two-qubit Heisenberg XYZ model. *International Journal of Quantum Information, 2, 393-405.*

[27] Androvitsaneas, P., Paspalakis, E., & Terzis, A., (2012). A quantum Monte Carlo study of the localizable entanglement in anisotropic ferromagnetic Heisenberg chains. *Annals of Physics, 327, 212-223.*

[28] Sinyagin, A., Belov, A., Tang, Z., & Kotov, N., (2006). Monte Carlo Computer Simulation of Chain Formation from Nanoparticles. *Journal of Physical Chemistry B, 110, 7500-7507.*

[29] Kim, I., (2013). Long-Range Entanglement is Necessary for a Topological Storage of Quantum Information. *Physical Review Letters, 111, 080503.*

[30] Elman, S., Bartlett, S., & Doherty, A., (2017). Long-range entanglement for spin qubits via quantum Hall edge modes. *Physical Review B, 96, 115407.*

[31] Bitko, D., Rosenbaum, T., & Aeppli, G., (1996). Quantum Critical Behavior for a Model Magnet. *Physical Review Letters, 77, 940-943.*

[32] Chakraborty, P., Henelius, P., Kjønsberg, H., Sandvik, A., & Girvin, S., (2004). Theory of the magnetic phase diagram of $LiHoF_4$. *Physical Review B, 70, 144411.*

[33] Bramwell, S., & Gingras, M., (2001). Spin Ice State in Frustrated Magnetic Pyrochlore Materials. *Science, 294, 1495-1501.*

[34] Castelnovo, C. R., & Sondhi, S., (2008). Magnetic Monopoles in Spin Ice. *Nature, 451, 42-45.*

[35] Mengotti, E., Heyderman, L., Bisig, A., Fraile Rodríguez, A., Le Guyader, L., Nolting, F., & Braun, H., (2009). Dipolar energy states in clusters of perpendicular magnetic nanoislands. *Journal of Applied Physics, 105, 113113.*

[36] Lahaye, T., Menotti, C., Santos, L., Lewenstein, M., & Pfau, T., (2009). The physics of dipolar bosonic quantum gases. *Reports on Progress in Physics. 72, 126401.*

[37] Peter, D., Müller, S., Wessel, S., & Büchler, H., (2012). Anomalous Behavior of Spin Systems with Dipolar Interactions. *Physical Review Letters, 109, 025303.*

[38] Islam, R., Senko, C., Campbell, W., Korenblit, S., Smith, J., Lee, A., Edwards, E., Wang, C., Freericks, J., & Monroe, C., (2013). Emergence and Frustration of Magnetism with Variable-Range Interactions in a Quantum Simulator. *Science, 340, 583-587.*

[39] Jurcevic, P., & Roos, C., (2014). Quasiparticle engineering and entanglement propagation in a quantum many-body system. *Nature, 511, 202-205.*

[40] Richerme, P., & Monroe, C., (2014). Non-local propagation of correlations in quantum systems with long-range interactions. *Nature, j511 pp. 198-201.*

[41] Mahmoudian S., Rademaker L., Ralko A., Fratini S., & Dobrosavljevic V., (2015). Glassy Dynamics in Geometrically Frustrated Coulomb Liquids without Disorder. *Physical Review Letters, 115, 025701.*

[42] Bohnet, J., Sawyer, B., Britton, J., Wall, M., Rey, A., Foss-Feig, M., & Bollinger, J., (2016). Quantum spin dynamics and entanglement generation with hundreds of trapped ions. *Science, 352, 1297-1301.*

[43] Sahling, S., & Lorenzo, E., (2015). Experimental realization of long-distance entanglement between spins in antiferromagnetic quantum spin chains. *Nature Physics, 15, 255-260.*

[44] Osborne, T., & Nielsen, M., (2002). Entanglement in a simple quantum phase transition. *Physical Review A, 66, 032110.*

[45] Vidal, G., Latorre, J., Rico, E., & Kitaev, A., (2003). Entanglement in Quantum Critical Phenomena. *Physical Review Letters, 90, 227902.*

[46] Bravo, B., Cabra, D., Gomez Albarracin, F., & Rossini, G., (2017). Long−range interactions in antiferromagnetic quantum spin chains. *Physical Review B, 96, 054441.*

[47] Duru, I.P., & Aktas, S., (2019). Localizable entanglement of isotropic antiferromagnetic spin-1/2 chain. *Turkish Journal of Physics. 43 pp. 272 - 279.*

[48] Bauer, B., Carr, L., Evertz, H., Feiguin, A., Freire, J., Fuchs, S., Gamper, L., Gukelberger, J., Gull, E., Guertler, S., Hehn, A., Igarashi, R., Isakov, S., Koop, D., Ma, P., Mates, P., Matsuo, H., Parcollet, O., Pawlowski, G., Picon, J., Pollet, L., Santos, E., Scarola, V., Schollwöck, U., Silva, C., Surer, B., Todo, S., Trebst, S., Troyer, M., Wall, M., Werner, P., & Wessel, S., (2011). The ALPS project release 2.0: open source software for strongly correlated systems. *Journal of Statistical Mechanics: Theory and Experiment, 2011, P05001.*

[49] DiVincenzo & Uhlmann, A., (1999). Entanglement of Assistance. *Quantum Computing and Quantum Communications, pp. 247-257.*

[50] Laustsen, T., Verstraete, F., & Van Enk, S., (2003). Local vs. Joint Measurements for the Entanglement of Assistance. *Quantum Information and Computation, 3, 64-83.*

[51] Popp, M., Verstraete, F., Martin-Delgado, M., & Cirac, J., (2005). Localizable entanglement. *Physical Review A, 71, 042306.*

[52] Todo, S., & Kato, K., (2001). Cluster Algorithms for General S Quantum Spin Systems. *Physical Review Letters, 87, 047203.*

[53] Vedral, V., & Plenio, M., (1998). Entanglement measures and purification procedures. *Physical Review A, 57, 1619-1633.*

[54] Qi, X., Gao, T., & Yan, F., (2017). Lower bounds of concurrence for N-qubit systems and the detection of k-nonseparability of multipartite quantum systems. *Quantum Information Process, 16, 23.*

[55] Xue-Na Zhu, M., & Fei, S., (2018). A lower bound of concurrence for multipartite quantum systems. *Quantum Information Processing, 17, 30.*

[56] Cornelio, M., (2013). Multipartite monogamy of the concurrence. *Physical Review A, 87, 032330.*